

Global consistency check of AIRS and IASI total CO₂ column concentrations using WDCGG ground-based measurements

Anyuan DIAO¹, Jiong SHU (✉)¹, Ci SONG¹, Wei GAO^{1,2,3}

¹ Key Laboratory of Geographic Information Science (Ministry of Education), School of Geographic Sciences, East China Normal University, Shanghai 200241, China

² Colorado State University, Department of Ecosystem Science and Sustainability, Fort Collins, Colorado 80523, USA

³ Colorado State University, Natural Resource Ecology Laboratory, Fort Collins, Colorado 80523, USA

© Higher Education Press and Springer-Verlag Berlin Heidelberg 2016

Abstract This article describes a global consistency check of CO₂ satellite retrieval products from the Atmospheric Infrared Sounder (AIRS) and Infrared Atmospheric Sounding Interferometer (IASI) using statistical analysis and data from the World Data Centre for Greenhouse Gases (WDCGG). We use the correlation coefficient (r), relative difference (RD), root mean square errors (RMSE), and mean bias error (MBE) as evaluation indicators for this study. Statistical results show that a linear positive correlation between AIRS/IASI and WDCGG data occurs for most regions around the world. Temporal and spatial variations of these statistical quantities reflect obvious differences between satellite-derived and ground-based data based on geographic position, especially for stations near areas of intense human activities in the Northern Hemisphere. It is noteworthy that there appears to be a very weak correlation between AIRS/IASI data and ten ground-based observation stations in Europe, Asia, and North America. These results indicate that retrieval products from the two satellite-based instruments studied should be used with great caution.

Keywords CO₂, consistency check, AIRS, IASI, WDCGG

1 Introduction

Carbon dioxide (CO₂), the dominant anthropogenic greenhouse gas and an indicator of climate change, has

dramatically increased from a pre-industrial level of 280 ppm (parts per million) to a current value of about 395 ppm, as described by the IPCC Fifth Assessment Report (AR5) (IPCC, 2014). This increase, which is mainly caused by human activities such as the burning of fossil fuels, has raised serious climate and sustainability concerns. It is expected that a further increase of atmospheric CO₂ will significantly alter future climate by affecting the Earth's radiation balance. It is essential to quantify variations in the temporal and spatial pattern of CO₂ concentrations in order to identify and understand sources and sinks at the Earth's surface and to better predict the influence of these factors on climate change.

Ground-based CO₂ observations and satellite measurements have provided the two main data sources for studying the variations in global atmospheric CO₂ concentrations. The World Data Centre for Greenhouse Gases (WDCGG) archives and provides data on CO₂ and other greenhouse gases measured mainly at surface stations. The WDCGG is one of the World Data Centres (WDCs) under the World Meteorological Organization's (WMO) Global Atmosphere Watch (GAW) program and, together with other programs, was created to provide information about variations in CO₂ and other greenhouse gases (WMO GAW Report No.161, 2005).

Several studies have been conducted to define the annual and seasonal changes of CO₂ based on measurements from ground-based stations. As a consistency check for CO₂ measurements from space, several publications have recently compared the Atmospheric Infrared Sounder (AIRS) retrieval products to WDCGG data from five ground-based stations using statistical techniques and have found that the AIRS data were in good agreement with the ground-based measurements (Bai et al., 2010; Zhou et al., 2013).

While traditional ground-based CO₂ measurements have a high accuracy and are collected continuously, spatial coverage is sparse and in certain areas, such as oceans and most parts of the Polar Regions, measurements are completely absent (Butz et al., 2009; O'Dell et al., 2012). Thus, it is impossible to accurately determine the sources and sinks of CO₂ based solely on ground-based measurements. Satellite sounders with various spatial, temporal, and spectral resolutions provide a unique opportunity to map atmospheric CO₂ globally.

Satellite measurements of global atmospheric CO₂ concentrations can fill the gaps between the ground-based measurements by providing daily global total CO₂ values and other products at a high spatial resolution. As the major satellite-based instruments for long time-series of high data quality, AIRS and the Infrared Atmospheric Sounding Interferometer (IASI) are a new generation of infrared instruments, providing observations using thousands of channels. The larger number of channels and the resulting diverse weighting functions imply that these sensors can achieve a higher resolution than the infrared sensors used earlier such as the High Resolution Infrared Radiation Sounder (HIRS). The ability of AIRS to track seasonal and latitudinal variations of CO₂ in the middle to upper troposphere has been verified by comparisons between AIRS data and NOAA Earth System Research Laboratory/Global Monitoring Division (ESRL/GMD) aircraft measurements carried out in 2005 (Maddy et al., 2008).

The IASI is an ideal sensor for studying the tropospheric CO₂ concentrations caused by biospheric emissions because of its daily, global, and complete spectral coverage across the thermal infrared region. It supplies monthly or weekly products that capture the natural variability of the Earth's surface (Hilton et al., 2012). It is important to validate the reliability of the retrieval products from AIRS and IASI against surface observational data from WDCGG using a variety of statistical methods. The observational records of WDCGG are chiefly related to the near-surface CO₂ concentrations, which closely reflect the column-averaged concentrations. Comparisons with values of satellite-derived CO₂ concentrations transported from the surface to the mid-troposphere also allow for space–time consistency checks despite different observational patterns and values for near-surface and space-based observations.

In this article we hope to clarify the similarities and differences between two kinds of total CO₂ column concentration data retrieved from AIRS and IASI. The results can be applied to climate studies with caution, as there are statistical discrepancies.

This article is organized as follows: Section 2 introduces the CO₂ data obtained from AIRS and IASI satellite observations and WDCGG ground-based measurements, Section 3 describes the statistical and analytical methodology, Section 4 presents the results and discussion, and conclusions are summarized in Section 5.

2 Data

2.1 Satellite observations

Two satellite-derived CO₂ datasets are examined in this study. These particular datasets are chosen because they provide free tropospheric column-averaged concentration information as well as scope for wide horizontal sampling. The first dataset is retrieved from AIRS, which is a cross-track scanning grating spectrometer that measures 2378 channels covering spectral ranges of 649–1136, 1217–1613, and 2181–2665 cm⁻¹. The AIRS instrument also includes four visible/near-IR(Vis/NIR) channels between 0.40 μm and 0.94 μm, with a 2.3-km FOV(Aumann et al., 2003). AIRS applies a spatial coherence quality assurance (QA) test, and the Level 2 CO₂ standard product consists of the retrievals that satisfy the acceptance criterion (Olsen et al., 2007; Olsen, 2009). Level 2 (L2) CO₂ products are retrieved using a Vanishing Partial Derivative (VPD) algorithm with a spatial resolution of 90 km × 90 km (Chahine et al., 2005). Level 3 (L3) CO₂ products are monthly data gridded at a 2.5° × 2° grid cell size and derive from L2 CO₂ products. We use Version 5, Level 3 monthly product data provided by the NASA Goddard Earth Sciences Data and Information Services Center (DISC).

The second dataset is obtained from IASI, which is a cross-track scanning Michelson interferometer that measures 8461 channels in the infrared (IR) range at 0.25 cm⁻¹ spacing between 645–2760 cm⁻¹(3.6–15.5 μm). The IASI has 30 ground fields of regard (FOR) per scan, each measuring a 2 × 2 array of footprints, which corresponds to a ground resolution of 12 km at nadir and a satellite altitude of 819 km (Schlüssel et al., 2005; Hilton et al., 2012). The IASI on Metop-A (Meteorological operational satellite-A) is the first in a series of three identical infrared interferometers planned to provide over 15 continuous years of data. Metop-B was declared fully operational and pronounced to replace Metop-A in April 2013. Metop-C is scheduled for launch toward the end of 2016. The IASI instrument has the potential to provide high-quality data, so it is crucial to characterize the quality of its retrievals.

2.2 Parameters of advanced sounders: AIRS, IASI, GOSAT, and SCIMACHY

AIRS and IASI are IR sounders which mainly work in the thermal infrared spectral region with maximum sensitivity in the middle to upper troposphere (Chalon et al., 2001; Phulpin et al., 2002; Aumann et al., 2003). GOSAT, based on near infra-red sounders (NIR) and SCIMACHY, based on short wave infra-red sounders (SWIR), have almost constant sensitivity to the entire atmosphere column with the maximum value near the surface, and are frequently used to derive the column-averaged dry air mole fractions of CO₂ in the atmosphere (XCO₂) (Bovensmann et al.,

1999; Kuang et al., 2002; Christi and Stephens, 2004; Buchwitz et al., 2005a, b; Kuze et al., 2009; Wang et al., 2012). For more details among these four sounders, please refer to the Table 1 below.

The NIR/SWIR sounders cannot collect data during night time, thus IASI and AIRS as IR sensors are crucial to provide data to construct a consistent long-term time series of atmospheric CO₂ observations from space (Wang et al., 2012). Since all of the instruments mentioned above operate in the optical spectral region (< 16 μm), their abilities to monitor atmospheric CO₂ are significantly limited by the presence of clouds. AIRS and IASI's performances are expected in places where radiometric measurements will be operable, like collecting data from areas where there is clear or partly cloudy sky. IASI's global coverage of the sounding system is ensured by the simultaneous use of the microwave sounder AMSU-A (Advanced Microwave Sounding Unit A). The AIRS spectrometer is designed to operate synchronously with the microwave instruments AMSU-A1 and AMSU-A2. Therefore, IASI/AIRS are much more suitable for checking global consistency than other sounders like GOSAT or SCIMACHY. For this reason we choose AIRS and IASI for checking their consistency with WDCGG.

In this study, we used Level 2 IASI retrievals product data provided by the NOAA National Environmental Satellite, Data, and Information Service (NESDIS) Center. The IASI CO₂ products are retrieved from NOAA's Comprehensive Large Array-data Stewardship System (CLASS) (<http://www.class.ngdc.noaa.gov>). For IASI Level 2 product, the columns of N₂O, CH₄, and CO₂ are

retrieved using artificial neural networks (ANN) trained with synthetic radiances (using RTTOV) and a collection of trace gas profiles from the MOZART model (Chalon et al., 2001). Additional details about IASI Level 2 products can be found in the IASI Level 2 Product Guide.

As for the resolution of IASI, the elementary (or effective) field of view (EFOV) is the useful field of view at each scan position. Each EFOV consists of a 2 × 2 matrix of instantaneous fields of view (IFOV). Each IFOV has a diameter of 14.65 millirad (mrad). Each IFOV corresponds to a ground resolution of 12 km at nadir and a satellite altitude of 819 km. The 2 × 2 matrix is centered on the viewing direction (IASI Level 2 Product Guide). Details of the IASI's data are show in Table 2; all these values and information are from its head files of IASI level 2 products.

2.3 Ground-based measurements

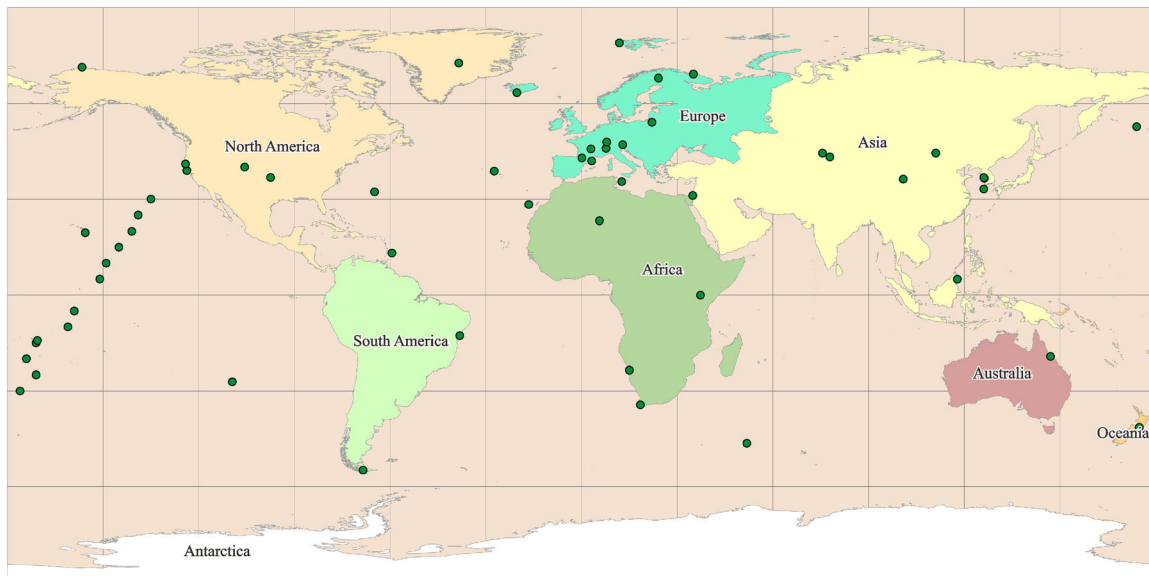
For this study, WDCGG ground-based measurement data are selected. WDCGG, first established in 1990, has been operating for more than 20 years. The data center gathers, archives, and provides data on CO₂, CH₄, CFCs, N₂O, O₃, and associated gases such as CO and NO_x for the atmosphere and oceans, as observed by GAW and other programs. The WDCGG data are based on a total of 132 CO₂ measurements at 114 stations. Monthly mean data from air sample observations at stationary platforms, collected from September 2008 to December 2010, are used in this article. The locations of the stations used in this study are shown in Fig. 1.

Table 1 The parameters of advanced sounders: AIRS, IASI, GOSAT, and SCIMACHY

| Parameter | Advanced Sounder | | | |
|--|--|---|--|--|
| | AIRS | IASI | GOSAT | SCIMACHY |
| Available trace gases in the troposphere | CO ₂ , CH ₄ , O ₃ , CO, H ₂ O, SO ₂ | CO ₂ , CH ₄ , O ₃ , CO, H ₂ O, SO ₂ , N ₂ O | CO ₂ , CH ₄ , O ₂ , O ₃ , H ₂ O | O ₃ , O ₄ , N ₂ O, CH ₄ , CO, CO ₂ , H ₂ O, SO ₂ , HCHO |
| Sensor | Infrared Sensor (IR) | Infrared Sensor (IR) | Near Infrared Sensor (NIR) | short wave Infrared Sensor (SWIR) |
| Instrument type | Grating Spectrometer | Interferometer | Cloud and Aerosol Imager and near infrared/SWIR radiometer | NIR channel 8 from nadir measurements |
| Observation strategy | Nadir | Nadir | Nadir, target | Limb, nadir |
| Spectral range/μm | 3.74–4.61 6.20–8.22 8.80–15.4 | 3.62–5.0 5.0–8.26 8.26–15.5 | 0.758–0.775 1.56–1.72 1.92–2.08 5.56–14.3 | 0.24–0.44 0.4–1.0 1.0–1.7 1.94–2.04 2.265–2.38 |
| Nominal altitude/km | 705 | 819 | 666 | 790 |
| Local time | 13:30 | 21:30 | 13:00±0:15 | 10:00 |
| Nominal launch date | May 2002 | October 2006 | January 2009 | March 2002 |
| Lifetime/year | 7 | 5 | 5 | 7 |

Table 2 IASI Level 2 products name-lists and the units (with NetCDFdata format)

| Type | Units | Type | Units |
|--|---------------|--|--------|
| The index of the AMSU FOV | none | Microwave surface class | none |
| UTC Milliseconds since Jan 1, 1970 | msec | Microwave surface emissivity | none |
| Retrieval latitude values for each AMSU FOV | degrees North | Number of MW spectral points AMSU FOV | none |
| Retrieval longitude values for each AMSU FOV | degrees East | Number of surface emis hinge points per AMSU FOV | none |
| View angle for each AMSU FOV | degrees | Number of cloud emis hinge points per AMSU FOV | none |
| Satellite height above each AMSU FOV | km | Number of cloud layers per AMSU FOV | none |
| Column averaged CO ₂ per AMSU FOV | ppm | Quality flags for retrieval | none |
| Solar zenith angles for each AMSU FOV | degrees | Ispare diagnostics array from retrieval | none |
| Ascending_Descending | none | Rspare diagnostics array from retrieval | none |
| Surface height | meters | Cloud top pressure | mb |
| Land fraction | none | Cloud top fractional coverage | none |
| Surface pressure | mb | Pressure | mb |
| Skin_Temperature | Kelvin | Effective_Pressure | mb |
| Skin temperature from MIT retrieval | Kelvin | Effective_Pressure | Kelvin |
| Skin temperature from the first guess | Kelvin | Temperature from MIT retrieval | Kelvin |
| | | Temperature from the first guess | Kelvin |

**Fig. 1** Geographical distribution of WDCGG ground-based stations (green dots), selected for consistency check with IASI and AIRS total CO₂ datasets.

3 Methodology

The evaluation indicators include correlation coefficient (r), relative difference (RD), root mean square errors (RMSE), and mean bias error (MBE). The correlation coefficient is the most important and useful statistical parameter to evaluate a relationship between two variables. In order to reduce the number of samples, the t -distribution is used to test the significant correlation coefficients. The

correlation coefficient is calculated by Eq. (1):

$$r_{xy} = \frac{\sum_{i=1}^N (x_i - \bar{x})(y_i - \bar{y})}{\sqrt{\sum_{i=1}^N (x_i - \bar{x})^2 \sum_{i=1}^N (y_i - \bar{y})^2}}, \quad (1)$$

where N is the number of samples, x_i represents the value of x for the sample i , i.e., the CO₂ data measured at ground-based stations, y_i represents the value of y for the sample i , i.e., the retrieved CO₂ value from one of the satellite

datasets, \bar{x} is the mean value for all x_i , and \bar{y} is the mean value for all y_i . The relative difference (RD) is calculated by Eq. (2):

$$RD_i = \frac{y_i - x_i}{x_i} \times 100\%, \quad (2)$$

where y_i and x_i represent the retrieved CO₂ values from satellite and ground-based observations, respectively, for sample i . The RMSE is often used to quantify the difference between an estimated value and the actual measured value. In this study, RMSE is calculated by the following equation (Eq. (3)):

$$RMSE = \sqrt{\frac{1}{N} \sum_{i=1}^N (y_i - x_i)^2}. \quad (3)$$

The MBE is calculated by the following equation (Eq. (4)):

$$MBE = \frac{1}{N} \sum_{i=1}^N RD_i, \quad (4)$$

where RD_i is the relative difference for the sample i .

4 Results and discussion

4.1 Consistency check of spatial variations between AIRS/IASI and WDCGG

The accuracy of retrieval products from space not only depends to a large degree on the method and algorithm used, but also appears to reflect both geographical environment and human activities (Zhou et al., 2013). Figure 2 shows that seven inland WDCGG stations, with corresponding regions of CO₂ data products from space (Table 3), show lower correlation coefficients. Two other maritime stations are also close to 0.5, assuming 0.5 to be the lower threshold limit. The reasons for these results could be attributed to the following aspects. First, the surface variation from ocean to land has a marked impact on the precision of the data retrieved from space.

Temperature, water vapor, and O₃ have great influence on the sensitivity of the atmospheric CO₂ data retrieval from the satellite observations. Water vapor is the most important factor in the tropical regions, whereas temperature creates a major interference for midlatitude and subarctic regions (Zhou et al., 2014). Second, for *in situ* measurements, the irregular turbulent transportation by the complex underlying surface, human activities, and adverse synoptic patterns disturb the effectiveness of the existing surface observations. The weaker relationship between CO₂ data products from space and *in situ* observation in heterogeneous terrestrial environments probably could be understood.

The analogy with this study has been presented by Olsen: the results showed that the land/ocean difference in the north-south gradient of the CO₂ concentration was greater than two times (11.2 ppm vs. 4.7 ppm) (Olsen and Randerson, 2004). Grieco et al. (2013) carried out a comparison in his study, to compare the IASI and AIRS retrieved CO₂ content averaged over the whole period of July 2010 for observations above the Mediterranean Sea. It is evident that the AIRS CO₂ products map display all the elements of random behavior and the IASI is in agreement with both the cycle and trend. Hence, the consistency check between satellite data and WDCGG ground-based observations with a large sample sizes can provide a more robust result as compared to the use of a single data source alone.

For the majority of stations located between 55°S and 80°N, the correlation coefficients vary from 0.1 to about 0.9. Statistical results indicate that 23% of the correlation coefficients between IASI and ground-based WDCGG observations are below 0.5, 48% are between 0.5 and 0.8, and 29% are above 0.8 (Fig. 3(a)). In contrast, 44% of the correlation coefficients for AIRS and ground-based WDCGG observations are below 0.4, 43% range between 0.4 and 0.8, and 13% are above 0.8.

From the variation of the two kinds of correlation coefficients with latitude, it can be found that correlation coefficients decrease with increasing latitude between AIRS and ground-based observations in the Northern

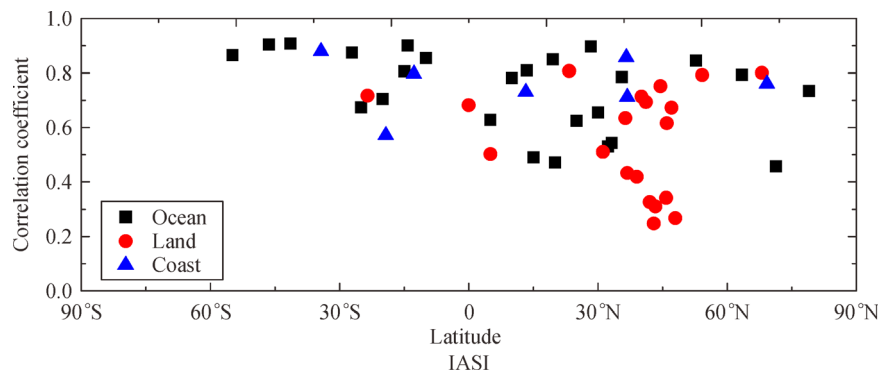


Fig. 2 Correlation coefficient variations for IASI products and WDCGG stations plotted against latitude.

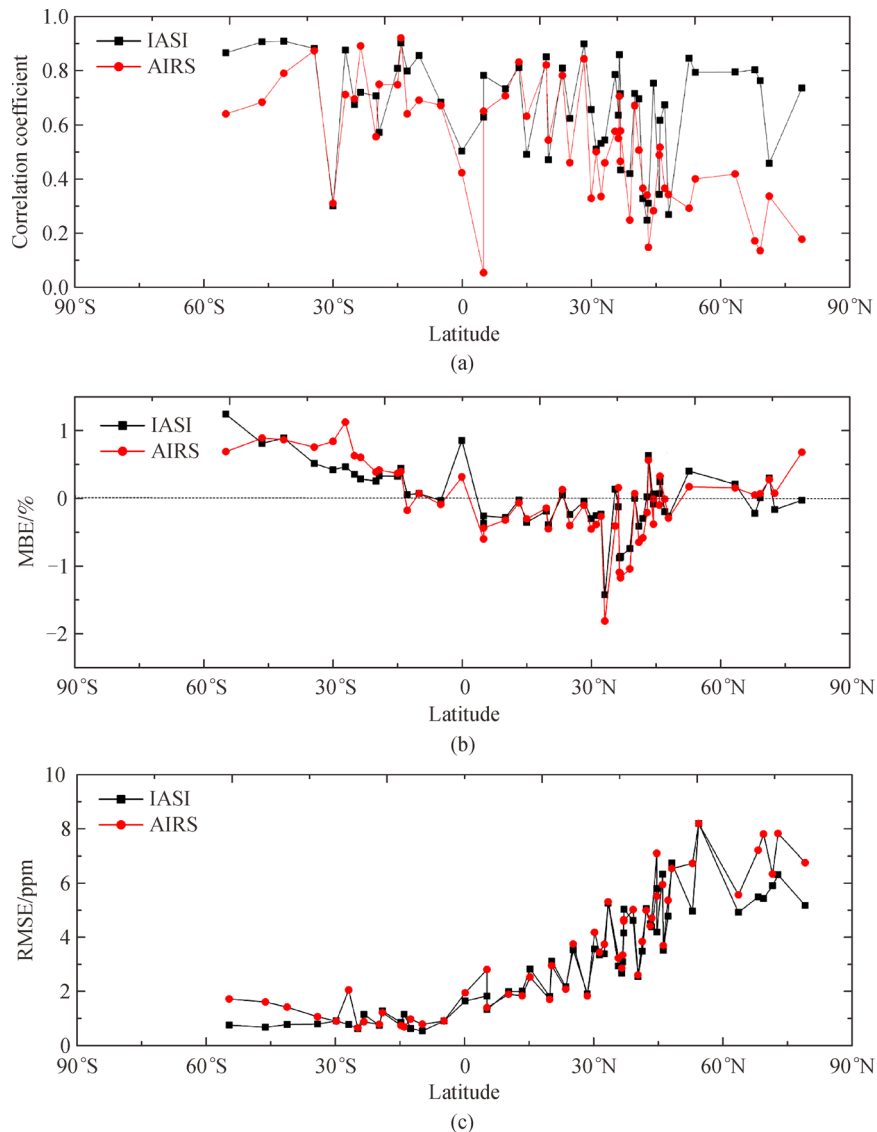
Table 3 Low correlation coefficients for ground-based observations and retrieval products from IASI over inland areas

| Station name | Latitude | Longitude | Altitude/m | Country | Correlation coefficient |
|-----------------------|-----------|-----------|------------|---------|-------------------------|
| Southern Great Plains | 36.78°N | 97.5°W | 314 | USA | 0.43319 |
| Point Arena | 38.95°N | 123.72°W | 17 | USA | 0.41907 |
| Begur | 41.97°N | 3.23°E | 13 | Spain | 0.32707 |
| Pic du Midi | 42.9372°N | 0.1411°E | 2877 | France | 0.24789 |
| Plateau Assy | 43.25°N | 77.87°E | 2519 | France | 0.3104 |
| Puy de Dome | 45.7719°N | 2.9658°E | 1465 | France | 0.34257 |
| Schauinsland | 47.92°N | 7.92°E | 1205 | Germany | 0.26769 |

Hemisphere, the values fall significantly north of 40°N. However the IASI correlation coefficients do not show a similar tendency with latitude, except for a slight downward trend from 55°S to 80°N. This variation tendency implies that accuracy of the retrieval products from space

not only is restricted by the method and algorithm used, but also appears to be under the influence of both the geographical environment and human activities, which also indirectly impact the quality of data retrieved.

Relative to Fig. 3(a), the MBE ($\leq 0.5\%$) for both IASI

**Fig. 3** Variations in (a) correlation coefficient, (b) MBE, and (c) RMSE with latitude for the AIRS, IASI, and WDCGG data.

and AIRS shows a decreasing consistency between the satellite-retrieved data and ground-based observations for 55°S–30°N, after which an increasingly undulant trend emerges (Fig. 3(b)). Figure 3(c) shows the RMSE for the two kinds of data gradually increases with latitude and reaches 8 ppm at about 50°N. Above 50°N, IASI shows a smaller deviation from the WDCGG CO₂ station data, although both sets of retrieved values begin to decrease from 50°N to 85°N (Fig. 3(c)).

4.2 Consistency check of seasonal variations between AIRS/IASI and WDCGG

To evaluate the long-term trends of the total CO₂ column concentrations, the monthly mean RD for retrieved CO₂ values versus ground-based observations from August 2008 to December 2010 are shown in Fig. 4. For a consistency check, different latitude zones are shown separately for the Northern and Southern Hemispheres. The statistical results indicate that the amplitude of RD fluctuations in the Northern Hemisphere for both AIRS and IASI gradually decreases with latitude and shows obvious seasonal characteristics. We tend to attribute these phenomena to CO₂ flux transportation from different latitude zones in the Northern Hemisphere. Regular photosynthesis in middle and high latitudes results in a greater amplitude of RD fluctuations because of obvious seasonal changes, however the amplitude weakens gradually in the tropical regions of low latitudes. The highest values for monthly mean CO₂ near the surface occur in winter, because reduced plant photosynthesis and fossil fuel combustion result in an accumulation of CO₂ near the surface. With the coming of spring (April and May), the RD begins to increase gradually, CO₂ retrieval values from space gradually rise, and the values near the surface fall by flux transportation. This vertical exchange of CO₂ will continue as the climate gradually warms until the maximum retrieval value appearance from space in

summer. The same argument explains why the highest values of RD occur in July to September: CO₂ retrieval values attain the maximum in the upper troposphere and lower stratosphere (UT, LS) by flux transportation because the minimum value of CO₂ concentrations near the surface is caused by enhanced carbon fixation.

It is therefore easy to understand why the RD is gradually reduced from autumn until the minimum in winter: CO₂ values from ground-based observations gradually increase after July through September with weakening carbon fixation, whereas CO₂ values retrieved from space begin to decrease again. It is obvious that the seasonal cycle of CO₂ is driven by biospheric respiration and transportation (Gerbig et al., 2003; Tiwari et al., 2006).

In the Southern Hemisphere, RD showed small amplitudes compared with the Northern Hemisphere by the terrestrial biosphere in the vast ocean.

4.3 Abnormal regions

It is noteworthy that there was a significant difference in the correlation coefficients between the AIRS/IASI retrieval products and the CO₂ recordings for ten of the WDCGG stations (Table 4). These differences are apparent for stations in Europe, Asia, and North America. The consistency check results for these correlation coefficients imply that the retrieval products from both AIRS and IASI for these regions should be used with great caution (Table 4).

5 Conclusions

In this article, the reliability of CO₂ retrieval products from AIRS and IASI relative to WDCGG ground-based measurements are examined employing frequently used statistical methods.

Both the CO₂ retrieval data and the corresponding

Table 4 Abnormal correlation coefficients for ground-based observations and retrieval products from IASI and AIRS for ten stations in Europe, Asia, and North America

| Station name | Latitude | Longitude | Altitude/m | Country | Correlation coefficient | |
|-----------------------------------|----------|-----------|------------|--------------------|-------------------------|----------|
| | | | | | IASI | AIRS |
| Danum Valley GAW baseline station | 4.97°N | 117.83°E | 426 | Malaysia | 0.627492 | 0.053252 |
| Pacific Ocean (30°N) | 30°N | 135°W | 10 | N/A | 0.655413 | 0.327731 |
| Tae-ahn Peninsula | 36.72°N | 126.12°E | 20 | Republic of Korea | 0.712489 | 0.464544 |
| Ulaan Uul | 44.45°N | 111.08°E | 914 | Mongolia | 0.751756 | 0.281842 |
| Shemya Island | 52.72°N | 174.08°E | 40 | USA | 0.843974 | 0.291524 |
| Puszcza Borecka/Diabla Gora | 54.15°N | 22.07°E | 157 | Poland | 0.791776 | 0.400088 |
| Heimaey | 63.4°N | 20.28°W | 100 | Iceland | 0.792858 | 0.418004 |
| Pallas-Sammaltunturi | 67.97°N | 24.12°E | 560 | Finland | 0.800925 | 0.17097 |
| Teriberka | 69.2°N | 35.1°E | 40 | Russian Federation | 0.761182 | 0.135397 |
| Zeppelinfjellet (Ny-Alesund) | 78.9°N | 11.88°E | 475 | Norway | 0.734377 | 0.176992 |

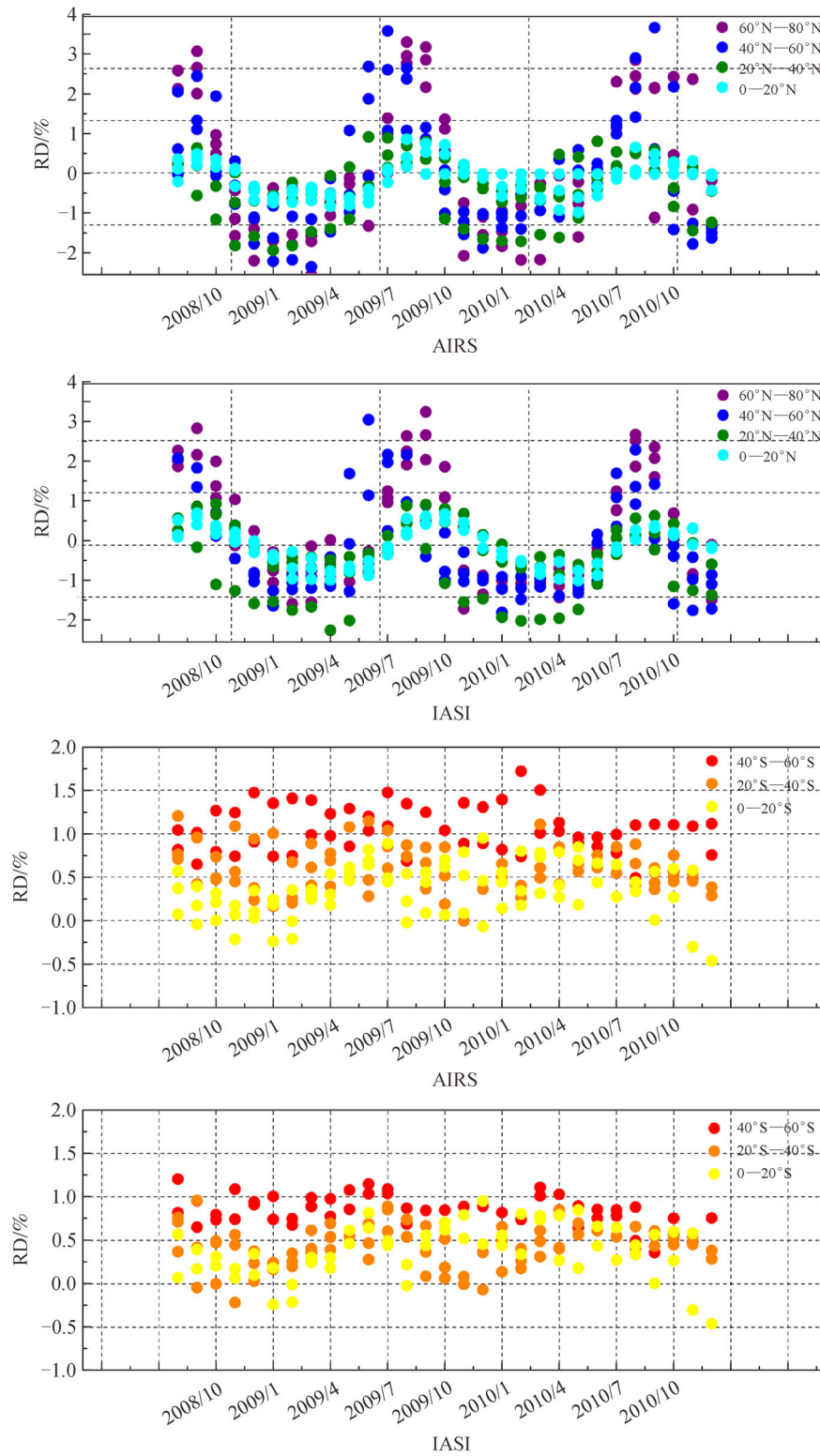


Fig. 4 Monthly mean RD between AIRS/IASI and WDCGG for the retrieved CO₂ concentrations versus the ground-based observations in the Northern and Southern Hemispheres from August 2008 to December 2010.

ground-based measurements correlate well within a region between 55°S and 30°N. In addition, the MBE and RMSE also indicate satisfactory accuracy. However, for stations located north of 30°N, correlation coefficients, MBE, and RMSE show significant differences between the two satellite-based measurements, probably caused by human activities. The seasonal CO₂ maximum in the UT and LS is caused by an accumulation of CO₂ in the boundary layer due to plant photosynthesis, fossil fuel combustion, and vertical transportation. The observed seasonal fluctuation of monthly mean RD is brought about by a hysteresis effect creating synchronous differences at different altitudes.

The consistency check for some of the correlation coefficients imply that data from AIRS and IASI retrieval products for several regions should be used with great caution.

Acknowledgements This project was supported by the National Basic Research Program of China (No. 2010CB951603) and the Major Program of National Social Science Foundation of China (No.13&ZD161). We thank Prof. Jietai Mao of the Department of Atmospheric & Oceanic Sciences, Peking University, China for providing expert advice and assistance. We also thank the WDCGG for providing the CO₂ data. Many thanks to NASA for providing AIRS CO₂ data and NOAA for providing IASI CO₂ data.

References

- Aumann H H, Chahine M T, Gautier C, Goldberg M D, Kalnay E, McMillin L M, Revercomb H, Rosenkranz P W, Smith W L, Staelin D H, Strow L L, Susskind J (2003). AIRS/AMSU/HSB on the aqua mission: design, science objectives, data products, and processing systems. *IEEE Trans Geosci Rem Sens*, 41(2): 253–264
- Bai W G, Zhang X Y, Zhang P (2010). Temporal and spatial distribution of tropospheric CO₂ over China based on satellite observations. *Chin Sci Bull*, 55(31): 3612–3618
- Bovensmann H, Burrows J P, Buchwitz M, Frerick J, Noël S, Rozanov V V, Chance K V, Goede A P H (1999). SCIAMACHY: mission objectives and measurement modes. *J Atmos Sci*, 56(2): 127–150
- Buchwitz M, de Beek R D, Burrows J P, Bovensmann H, Warneke T, Notholt J, Meirink J F, Goede A P H, Bergamaschi P, Körner S, Heimann M, Schulz A (2005a). Atmospheric methane and carbon dioxide from SCIAMACHY satellite data: initial comparison with chemistry and transport models. *Atmos Chem Phys*, 5(4): 941–962
- Buchwitz M, de Beek R, Noël S, Burrows J P, Bovensmann H, Bremer H, Bergamaschi P, Körner S, Heimann M (2005b). Carbon monoxide, methane and carbon dioxide columns retrieved from SCIAMACHY by WFM-DOAS: year 2003 initial data set. *Atmos Chem Phys*, 5(12): 3313–3329
- Butz A, Hasekamp O P, Frankenberg C, Aben I (2009). Retrievals of atmospheric CO₂ from simulated space-borne measurements of backscattered near-infrared sunlight: accounting for aerosol effects. *Appl Opt*, 48(18): 3322–3336
- Chahine M, Barnet C, Olsen E T, Chen L, Maddy E (2005). On the determination of atmospheric minor gases by the method of vanishing partial derivatives with application to CO₂. *Geophys Res Lett*, 32(22): L22803
- Chalon G, Cayla F, Diebel D (2001). IASI: an advanced sounder for operational meteorology. In IAF, International Astronautical Congress, 52 nd, Toulouse, France
- Christi M J, Stephens G L (2004). Retrieving profiles of atmospheric CO₂ in clear sky and in the presence of thin cloud using spectroscopy from the near and thermal infrared: a preliminary case study. *Journal of Geophysical Research: Atmospheres* (1984–2012), 109(D4)
- Gerbig C, Lin J C, Wofsy S C, Daube B C, Andrews A E, Stephens B B, Bakwin P S, Grainger C A (2003). Toward constraining regional-scale fluxes of CO₂ with atmospheric observations over a continent: 1. Observed spatial variability from airborne platforms. *J Geophys Res*, D, Atmospheres, 108(D24): 4756
- Grieco G, Masiello G, Matricardi M, Serio C (2013). Partially scanned interferogram methodology applied to IASI for the retrieval of CO₂, CH₄ and N₂O. *Opt Express*, 21(21): 24753–24769
- Hilton F, Armante R, August T, Barnet C, Bouchard A, Camy-Peyret C, Capelle V, Clarisse L, Clerbaux C, Coheur P F, Collard A, Crevoisier C, Dufour G, Edwards D, Fajjan F, Fourrié N, Gambacorta A, Goldberg M, Guidard V, Hurtmans D, Illingworth S, Jacquinet-Husson N, Kerzenmacher T, Klaes D, Lavanant L, Masiello G, Matricardi M, McNally A, Newman S, Pavein E, Payan S, Péquignot E, Peyridieu S, Phulpin T, Remedios J, Schlüssel P, Serio C, Strow L, Stubenrauch C, Taylor J, Tobin D, Wolf W, Zhou D (2012). Hyperspectral earth observation from IASI: five years of accomplishments. *Bull Am Meteorol Soc*, 93(3): 347–370
- IPCC (2014). Climate Change 2014: Synthesis Report. Contribution of Working Groups I, II and III to the Fifth Assessment Report of the Intergovernmental Panel on Climate Change [Core Writing Team, R. K. Pachauri and L.A. Meyer (eds.)]. IPCC, Geneva, Switzerland, 151
- Kuang Z, Margolis J, Toon G, Crisp D, Yung Y (2002). Space borne measurements of atmospheric CO₂ by high-resolution NIR spectrometry of reflected sunlight: an introductory study. *Geophys Res Lett*, 29(15): 11-1–11-4
- Kuze A, Suto H, Nakajima M, Hamazaki T (2009). Thermal and near infrared sensor for carbon observation Fourier-transform spectrometer on the Greenhouse Gases Observing Satellite for greenhouse gases monitoring. *Appl Opt*, 48(35): 6716–6733
- Maddy E S, Barnet C D, Goldberg M, Sweeney C, Liu X (2008). CO₂ retrievals from the atmospheric infrared sounder: methodology and validation. *J Geophys Res*, D, Atmospheres, 113(D11): D11301
- O'Dell C W, Connor B, Bösch H, O'Brien D, Frankenberg C, Castano R, Christi M, Eldering D, Fisher B, Gunson M, McDuffie J, Miller C E, Natraj V, Oyafuso F, Polonsky I, Smyth M, Taylor T, Toon G C, Wennberg P O, Wunch D (2012). The ACOS CO₂ retrieval algorithm—Part 1: description and validation against synthetic observations. *Atmos Meas Tech*, 5(1): 99–121
- Olsen E T (2009). AIRS Version 5 Release Tropospheric CO₂ Products. Jet Propulsion Laboratory, California Institute of Technology, Pasadena, California
- Olsen E T, Fishbein E, Granger S, Lee S Y, Manning E, Weiler M, Blaisdell J, Susskind J. (2007). AIRS/AMSU/HSB Version 5 Data Release User Guide
- Olsen S C, Randerson J T (2004). Differences between surface and column atmospheric CO₂ and implications for carbon cycle research. *Journal of Geophysical Research: Atmospheres* (1984–2012), 109 (D2)

- Phulpin T, Cayla F, Chalon G, Diebel D, Schlüssel P (2002). IASI on board Metop: project status and scientific preparation. In 12th International TOVS Study Conference, Lorne, Victoria, Australia (Vol. 26)
- Schlüssel P, Hultberg T H, Phillips P L, August T, Calbet X (2005). The operational IASI level 2 processor. *Adv Space Res*, 36(5): 982–988
- Tiwari Y K, Gloor M, Engelen R J, Chevallier F, Rödenbeck C, Körner S, Peylin P, Braswell B H, Heimann M (2006). Comparing CO₂ retrieved from Atmospheric Infrared Sounder with model predictions: implications for constraining surface fluxes and lower-to-upper troposphere transport. *J Geophys Res, D, Atmospheres*, 111(D17): D17106
- Wang T, Shi J, Jing Y, Xie Y (2012). Investigation of the consistency of atmospheric CO₂ retrievals from different space-based sensors: intercomparison and spatiotemporal analysis. *Chin Sci Bull*, 58(33): 4161–4170
- WMO GAW Report No. 161 (2005). 12th WMO/IAEA Meeting of Experts on Carbon Dioxide Concentration and Related Tracers Measurement Techniques. Geneva: World Meteorological Organization
- Zhou C, Shi R, Liu C, Gao W (2013). A correlation analysis of monthly mean CO₂ retrieved from the Atmospheric Infrared Sounder with surface station measurements. *Int J Remote Sens*, 34(24): 8710–8723
- Zhou M, Shu J, Song C, Gao W (2014). Sensitivity studies for atmospheric carbon dioxide retrieval from atmospheric infrared sounder observations. *Journal of Applied Remote Sensing*, 8: 083697-2–083697-16